How to cite: *Angew. Chem. Int. Ed.* **2021**, *60*, 766–773
International Edition: doi.org/10.1002/anie.202011368
German Edition: doi.org/10.1002/ange.202011368

Phosphorus Heterocycles

En Route Towards the Control of Luminescent, Optically-Active 3D Architectures

*Philip Hindenberg, Frank Rominger, and Carlos Romero-Nieto**

Abstract: *π-Extended systems are key components for the development of future organic electronic technologies. While conceiving molecules with improved properties is fundamental for the evolution of materials science, keeping control over the 3D arrangement of molecules represents an ever-expanding challenge. Herein, a synthetic protocol to replace carbon atoms of π-systems by dissymmetric phosphorus atoms is reported; in particular, it allowed for conceiving new fused phosphapyrene derivatives with improved properties. The presence of dissymmetric phosphorus atoms precluded the formation of excimers. X-ray diffraction revealed that, meanwhile, strong intermolecular interactions are taking place in the solid state. The phosphapyrenes photoluminesce in the visible region with high quantum yields; importantly, they are CD-active. In addition, the unique non-planar features of phosphorus atoms allowed for the control of the 3D arrangement of molecules, rendering lemniscate-like structures. Based on our discoveries, we envisage the possibility to construct higher-order, chiral 3D architectures from larger phosphorus-containing π-systems.*

Modern organic chemistry has led to a rapid evolution of π-extended systems since they are pivotal for the development of future technologies. This is due to their capacity to absorb and (often) emit light, their accessible redox processes and/or their charge transport properties.[1] In the last years, scientists have devoted extensive research efforts to tailor the electronic properties of π-extended systems to particular applications.[1,2] Thus, important advances have been made in the bottom up synthesis of all-carbon architectures including nanoribbons,[3] acenes,[4] rylenes,[5] helicenes,[6] and truxenes.[7] However, conceiving molecules with new intriguing features is not sufficient. Intermolecular interactions ultimately define the magnitude of the molecular properties; luminescence, electronic and structural properties of the materials strongly depend on the spatial disposition of molecules. This has triggered a plethora of investigations towards the precise organization of molecules by means of either covalent,[8] non-covalent[9] or coordinative interactions.[10] Nevertheless, despite the progresses in the field, the development of strategies for controlling the 3D arrangement of molecules has become an everlasting scientific challenge.

In that context, pyrenes are a representative example of π-extended system in which the molecular arrangement has a strong impact on the molecular properties. Pyrene derivatives have focused the attention of researchers for decades because of their blue photoluminescence with high quantum efficiency;[11] however, they present two main drawbacks: a) pyrenes emit in the UV,[12] which is unsuitable for optical applications, and b) they have a high tendency to form excimers by intermolecular interactions already at low concentrations, leading to a broad, red-shifted emission with reduced quantum yield.[12,13] Thus, excimers are a hurdle task to overcome for luminescent purposes. Synthetic strategies have been proposed to circumvent excimer formation in π-extended systems including pyrenes; they mostly involve the decoration of the main framework with bulky functionalizations to preclude the intermolecular interactions[11a,14,15] However, despite a few exceptions, the latter strategy leads, among others, to randomly organized molecules.[14b,15,16] Thus, an ideal solution—also applicable to a variety of π-extended systems—would be to insert (hetero)atomic components into the main framework that could allow not only for the modulation of the properties but also for the control of the molecular arrangement, with the possibility to create well-defined 3D motifs. Notwithstanding, this concept remains underdeveloped.

In particular, despite the replacement of carbon atoms of pyrenes' core by other heteroatoms dates from the 1960s,[17] the use of phosphorus atoms in that context has received little attention. This is surprising. Phosphorus atoms present unique electronic and structural features to develop new strategies for tackling the above-mentioned ongoing challenges of π-extended systems: a) phosphorus centers may act as electron donors or acceptors,[18] and b) once embedded into π-systems, they accept up to two out-of-plane substituents,[19] fragments **E¹** and **E²** (Figure 1a), which in turn may impact the electronic properties through unique hyperconjugative effects.[18b,20] Notably, the **E¹** and **E²** substituents may be alkyl or aryl groups, halogens, transition metals or main-group elements among others.[18,19]

With the latter features in mind, we targeted to use the out-of-plane phosphorus substituents as vector directors to synergistically control the 3D organization of π-extended

[*] P. Hindenberg, Dr. F. Rominger, Priv.-Doz. Dr. C. Romero-Nieto
Ruprecht-Karls-Universität Heidelberg,
Organisch-Chemisches Institut
Im Neuenheimer Feld 270, 69120 Heidelberg (Germany)
E-mail: carlos.romero.nieto@oci.uni-heidelberg.de
Priv.-Doz. Dr. C. Romero-Nieto
Universidad de Castilla-La Mancha, Faculty of Pharmacy
Calle Almansa 14 – Edif. Bioincubadora, 02008, Albacete (Spain)
Supporting information and the ORCID identification number(s) for the author(s) of this article can be found under: https://doi.org/10.1002/anie.202011368.

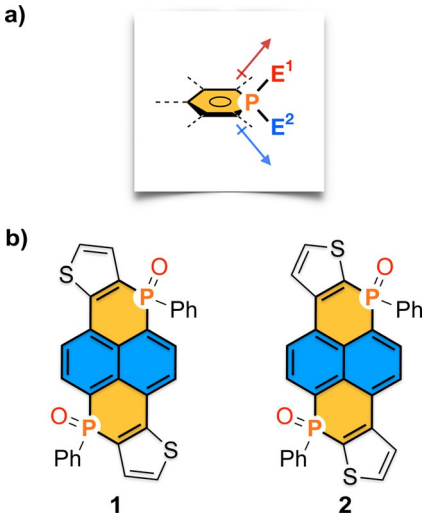

Figure 1. a) Representation of the phosphorus out-of-plane substituents **E¹** and **E²** as potential vector directors for building up well-defined 3D architectures. b) Designed novel phosphapyrenes **1** and **2**.

molecules while modulating the optoelectronic properties. In addition, utilizing two different out-of-plane substituents **E¹** and **E²** would afford dissymmetric phosphorus centers, which could potentially provide intrinsic optical activity to the π-systems (Figure 1a). It is noteworthy that luminescent optically active molecules are particularly attractive since they are key for the development of applications such as encrypted transport, anti-glare displays, optical communication, etc.;[21] they are consequently receiving increasing attention over the last few years.

The requirements for the precise organization of molecules are: a) the π-system must necessarily present more than one dissymmetric phosphorus atom, and b) the latter should not be invertible to keep control over the orientation of the π-system. Importantly, the number of available structures in literature with such particular characteristics is very limited.[19a,e] As a matter of fact, synthetic methodologies to replace carbon atoms in π-systems by dissymmetric phosphorus centers are rather scarce.

Thus, to demonstrate the feasibility of our concept, we designed the novel phosphapyrenes **1** and **2** (Figure 1b). Note that they contain two fused thiophenes through different patterns to investigate the influence of the latter rings into the molecular properties. Both molecules **1** and **2** possess two dissymmetric phosphorus centers as cornerstones for the construction of the 3D structures. For each out-of-plane **E¹** and **E²** phosphorus substituents, we chose an oxygen atom and a phenyl ring, respectively. P–O bonds are strongly polarized and could be potentially used as vector directors to link the molecular components by electrostatic non-covalent interactions through appropriate linkers.

The first bottleneck of our approach was the synthesis of **1** and **2**. To that end, we initially designed synthetic strategies **A** and **B** (Scheme 1); they involve a double cyclization from phosphine moieties placed either at the peripheral aromatic substituents (intermediate **5**) by electrophilic aromatic substitution (S_EAr) or at the naphthalene core (compound **9**) through metal-catalyzed reaction, respectively.

Strategy **A** was unsuccessful. Suzuki coupling at the 1,5-positions of the naphthalene derivative **3** with the corresponding aromatic rings, led to precursor **4** (see Supporting Information for details). However, subsequent double cyclization by S_EAr, that is, treatment of **4** with ^{t}BuLi at low temperature followed by the reaction with dichlorophenylphosphane,[22] did not lead to the targeted compounds **1** and **2**. Further optimizations by modifying the reaction temperature were fruitless. We then moved to strategy **B** (Scheme 1).

Here, the placement of the phosphine moieties at the naphthalene core (compound **9**), requires the preparation of the 1,5-dihalo intermediate **8**. We undertook its synthesis from the 1,5-dihydroxy derivative **6** (see Supporting Information for details). However, the 1,5-positions turned out to be highly unreactive. Direct halogenation of the hydroxy groups with Ph_3PBr_2, $POCl_3$, $POCl_3/PCl_5$, Ph_3PCl_2 or $PhPCl_4$ were unsuccessful to obtain molecule **8**. The transformation of the hydroxy moieties into good leaving groups such as SO_3H, OTf, $SC(O)NMe_2$ and $OC(O)CMe_3$ ultimately did not allow us to introduce the targeted halogen atoms into the 1,5-positions, either through nucleophilic aromatic substitution or by metal-catalyzed reactions. Importantly, reactions from the model compound naphthalene 1,5-ditriflate with, for example, $Pd_2(dba)_3$ and KBr under the same conditions utilized for **7** (**FG** = OTf) afforded the corresponding 1,5-dibromonaphthalene (see Supporting Information for details). This supports the deactivation of the 1,5-positions by the peripheral aromatic substituents; further investigation of this fact goes beyond the scope of this investigation and will be published elsewhere.

In view of the impossibility to access compound **9** through strategy **B**, we re-designed our approach to incorporate the phosphorus moieties into the 1,5-positions before the introduction of the peripheral aromatic substituents (strategy **C**, Scheme 1). Thus, we incorporated the diphenylphosphine oxide fragments from **10** by halogen-lithium interchange with ^{t}BuLi, reaction with chlorodiphenylphosphane and subsequent oxidation obtaining derivative **11**. The transformation of the methoxy groups of **11** into triflates (compound **13**) led to the required reactant to introduce the peripheral aromatic substituents (see Supporting Information for details). To this end, we chose thiophene moieties; they can be regioselectively functionalized through a variety of reactions, from lithiation to metal-catalyzed transformations. Whereas several attempts via Stille cross-coupling reactions with different conditions failed, double Suzuki coupling from **13** yielded compounds **14a**,**b** (Scheme 1) (see Supporting Information for details). The final step, the double cyclization, was critical. Taking into consideration the versatile reactivity of thiophenes towards C–H insertions,[23] we started considering reactions based on palladium-catalyzed P–C bond formations through direct C–H activation at the thiophene rings. The reaction would necessarily occur through a seven-membered P-Pd carbocycle (7MP-Pd),[24] even though the latter 7MP-Pd intermediates can hardly be found in literature.

To test the cyclization reaction, we first reduced the phosphorus centers of **14** with $HSiCl_3$ to yield **9a**,**b**. The

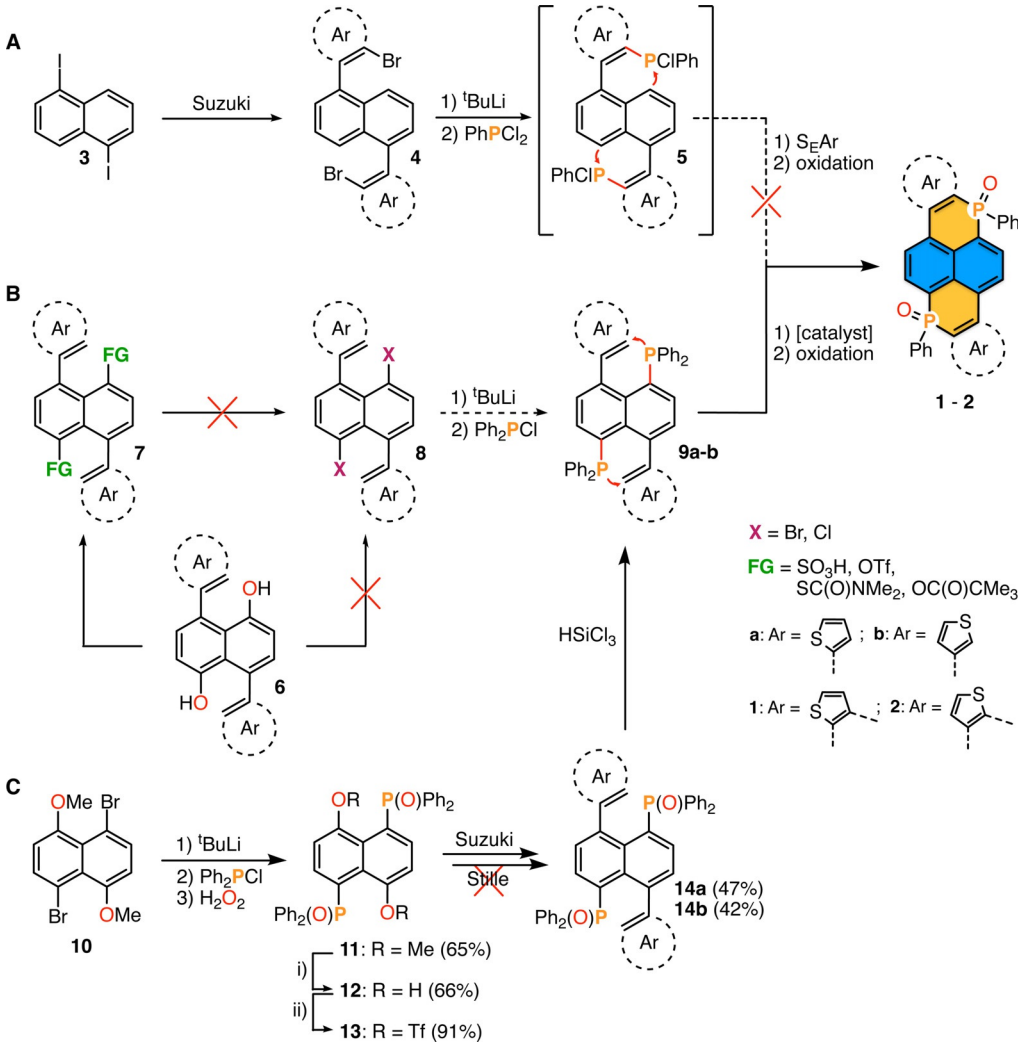

Scheme 1. Synthetic routes **A**, **B** and **C** for the preparation of phosphapyrenes **1** and **2**. i) BBr_3; ii) $PhNTf_2$, Et_3N, DMAP. **FG** = Functional Group. [Catalyst] = $Pd(OAc)_2$. See Supporting Information for details.

cyclization reaction turned out to be intriguing. The use of varying catalytic amounts of $Pd(OAc)_2$ (from 2 to 10 mol%), with different solvents (toluene or dimethylformamide) and reaction temperatures up to 130 °C did not lead to any ring closure; only the starting materials were detected in the reaction controls. However, after a long optimization process, we found out that the treatment of **9a**,**b** with 3.2 equivalents of $Pd(OAc)_2$ successfully led not only to close both phosphorus rings through direct C–H activation but also to cleave one of the phenyl substituents of the phosphorus atom; oxidation of the phosphorus centers took place during the standard reaction workup. As a result, we successfully obtained **1** and **2** with two dissymmetric phosphorus atoms; i.e., with the desired oxygen atom as vector director to construct 3D architectures. Importantly, both derivatives were photo- and air-stable; we did not observe any decomposition over months. Such a stability allowed us to separate the respective *cis*- and *trans*-isomers, that is, derivatives with the P-phenyl substituents either at the same or different planes of the molecule, by column chromatography. It is noteworthy that the phosphorus atoms did not invert even at temperatures up to 130 °C; a characteristic that was already observed in other phosphorus π-systems.[25]

The structures of the *cis*- and *trans*-isomers of compounds **1** and **2** obtained by X-ray diffraction are shown in Figure 2 (see Figures S1 to S4 for bond distances analyses). Indeed, all molecules present two dissymmetric phosphorus centers. Their molecular frameworks are planar, although the phosphorus atoms appear slightly out-of-plane (Figures S1 to S4). This was already observed in π-systems with cationic phosphorus centers.[26] Remarkably, the *cis*-isomers of **1** and **2** present similar packing in the solid state; the position of the sulfur atoms does not influence the molecular packing. Compounds **1**-*cis* and **2**-*cis* intercalate with each other with π-π distances of 3.36 and 3.32 Å, respectively (Figures 2, S1 and S3). Thus, strong phosphapyrene-phosphapyrene interactions are observed in the solid state. On the contrary, while **1**-*trans* also presents intercalated molecules with π-π distances of 3.39 Å, **2**-*trans* displays slipped π-stacks arranged along one axis and herringbone pattern between stacks (Figure 2).

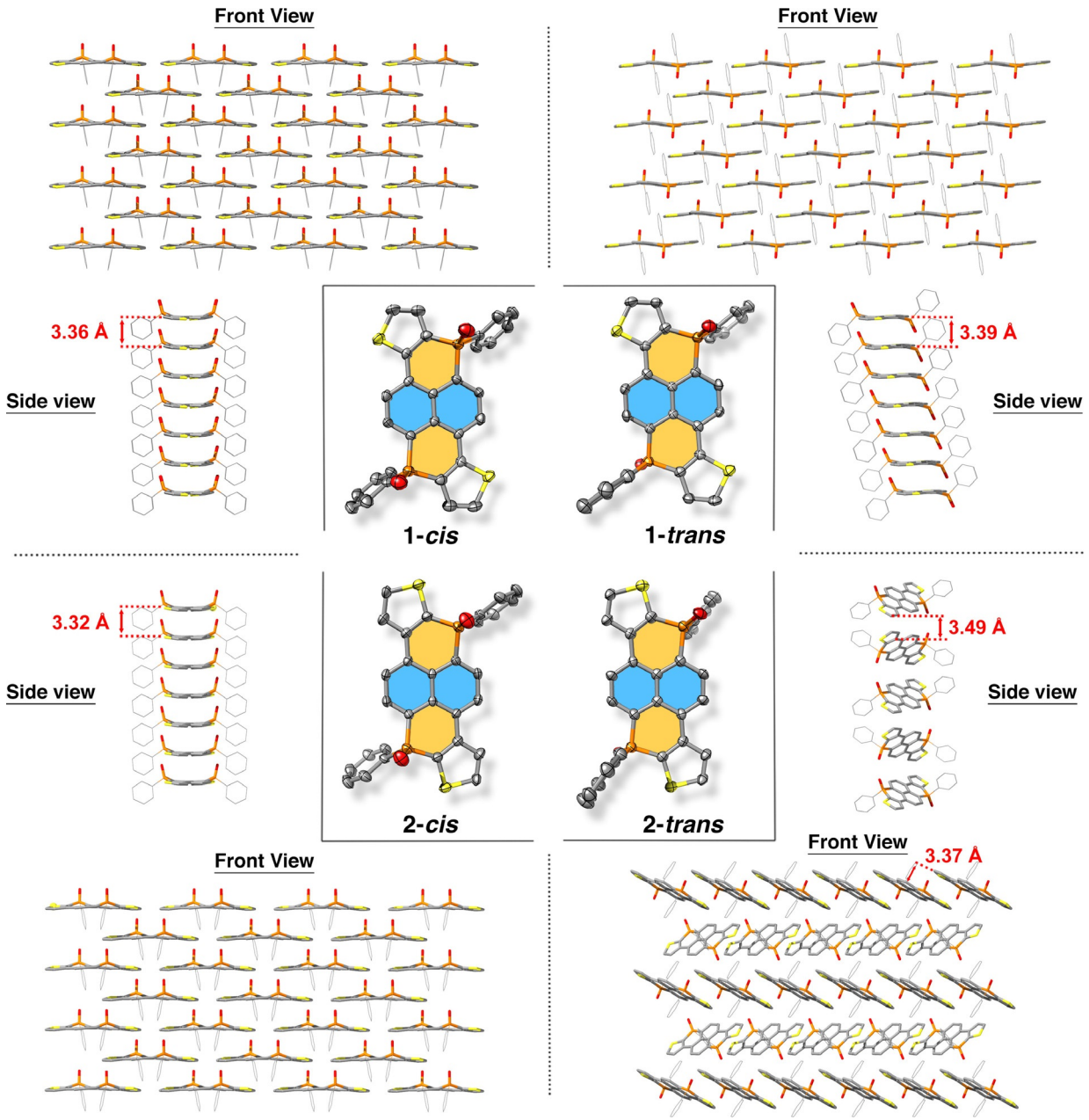

Figure 2. X-Ray structures of **1**-*cis*, **1**-*trans* and **2**-*cis*, **2**-*trans*. Numbers in red indicate intermolecular distances in angstrom.

Initial investigations on the electronic properties of the phosphapyrenes came from DFT calculations at the B3LYP/6-311 + G(d) level of theory. In agreement with the X-ray structures, all optimized geometries are essentially planar. HOMO and LUMO appear homogeneously distributed over the entire surface including the phosphorus atoms (Figure 3 a and S5). This points to an efficient electronic delocalization of the frontier molecular orbitals along the phosphapyrene structures. Even though the differences are rather small, the HOMO and LUMO energies from the *cis*- and *trans*-derivatives of **1** and **2** vary slightly (Table S3). This may be attributed to the proximity of the phenyl P-substituents in the *cis*-molecules. Compounds **1**-*cis* and **1**-*trans*, present a LUMO energy at −2.94 eV and HOMO energies at −6.21 and −6.20 eV, respectively (Table S3). In turn, the LUMO energies of **2**-*cis* and **2**-*trans* are at −2.83 and −2.84 eV, whereas the HOMO energies are −6.32 and −6.3 eV, respectively. These values are in stark contrast with the frontier molecular orbital energies of pristine pyrene; LUMO and HOMO are −1.83 and −5.65 eV (Table S3, Figure S7). Thus, the band gap is remarkably reduced from 3.82 eV for the parent pyrene to 3.27 and 3.26 eV for **1**-*cis* and **1**-*trans*, and 3.48 and 3.46 eV for **2**-*cis* and **2**-*trans*. Extending the conjugation through the fused thiophenes could be the explanation. However, calculations of the dithiophene-fused pyrene analogues to **1** and **2** (fused pyrenes **1** and **2**, Figures S6) revealed that, while the LUMO is slightly reduced compared to the parent pyrene as a result of extending the conjugation from −1.83 to −1.98 eV for the

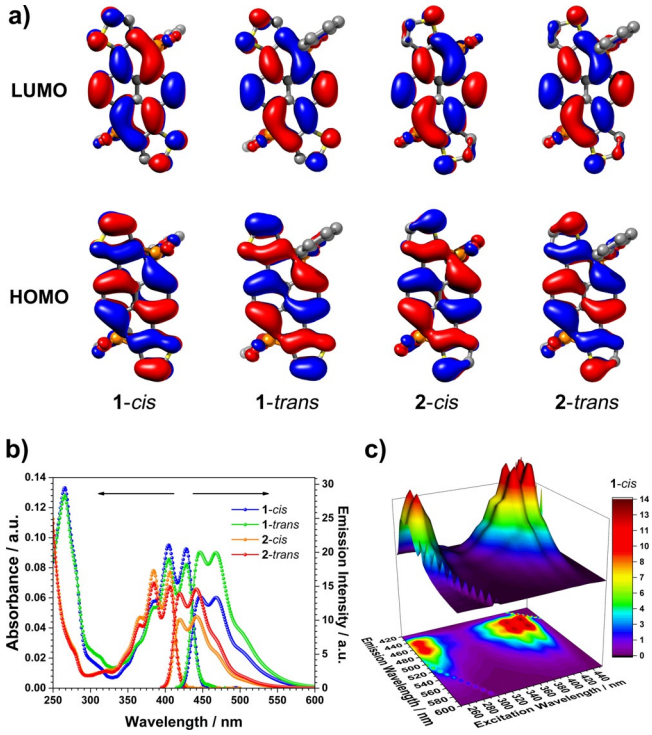

Figure 3. a) HOMO and LUMO distribution of **1** and **2**. b) Absorption and emission spectra of **1** and **2** from DCM solutions. c) 3D emission mapping of compound **1**-*cis*.

fused pyrene **1**, the enrichment of the pyrene core with further electronic density from the thiophene moieties increases the HOMO from −5.65 to −5.38 eV (Table S3). As evidenced in Figure S7, embedding two phosphorus atoms within the pyrene core appears, therefore, to be responsible for the pronounced reduction of LUMO and HOMO levels.

The energetic differences between **1** and **2** were corroborated by electrochemical measurements (Table S5 and Figures S8 and S9). In line with the theoretical calculations, the behavior of isomers *cis* and *trans* of compound **1** and **2** differed. All derivatives present an irreversible oxidation process; they maximize at 1.37 and 1.38 V for the **1**-*cis* and **1**-*trans*, and 1.26 and 1.36 V for **2**-*cis* and **2**-*trans*, respectively. The reduction processes are notably different. Compound **1**-*cis* shows a reversible reduction at −0.86 V[27] and a quasi-reversible reduction at −1.3 V. On the other hand, **1**-*trans* presents two irreversible reductions at −0.88 V and at −1.24 V (Figure S8). In turn, **2**-*cis* shows two quasi-reversible reductions at −0.98 and −1.45 V, and **2**-*trans* two irreversible ones at −0.95 and −1.43 V. The differences between isomers agree with distinct electronic reorganizations after the redox processes. All in all, it is worth highlighting that the presence of two phosphorus atoms converts the pyrene moieties into excellent electron acceptors reducing the reduction potential from −2.04 V for parent pyrenes[28] to c.a. −0.87 V and −0.97 for **1** and **2**, respectively.

Steady-state spectroscopy revealed a peculiar scenario. Typical absorption spectrum of genuine pyrene features three absorption bands in the UV at 308, 320 and 336 nm.[29] Following a comparable pattern, although red shifted, **1**-*cis* and **1**-*trans* exhibit maxima at 385, 405 and 428 nm with an additional high-energy band at 266 nm, whereas the absorption spectra of **2**-*cis* and **2**-*trans* maximize at 366, 385 and 406 nm (Figure S11 and Table S6). Estimations from TD-DFT calculations at the B3LYP/6-311 + G(d) level of theory assign a pure HOMO–LUMO transition for the lowest energetic bands; their corresponding theoretical λ_{max} fit quite well with the experimental values (Table S4 and Figure S10). The more energetic bands involve a combination of electronic transitions from different molecular orbitals (Table S4). Note that the latter combinations differ within the *cis* and *trans* derivatives. The theoretical λ_{max} of the more energetic absorption bands are however underestimated due to, presumably, the intrinsic limitation of the utilized theoretical base function.

In stark contrast with the parent pyrenes, the phosphapyrenes photoluminesce in the visible region of the electromagnetic spectrum (Figures 3 and S11 to S13); that is, the phosphorus atoms in combination with their two out-of-plane substituents lead to modulating the optical properties of the π-core. Diluted dichloromethane solutions of pristine pyrene present an emission spectrum in the UV that is characterized by three main vibrational peaks at 375, 385 and 397 nm.[30] In contrast, the emission features of **1** and **2** mirror-image the absorption spectra with prominent bands in the blue region of the visible spectrum; i.e., **1**-*cis* and **1**-*trans* display maxima at 446, 468 and 502 nm and derivatives **2**-*cis* and **2**-*trans* at 419, 443 and 469 nm (Figures 3b and S11 to S13). All derivatives were photostable. This allowed us to map the 3D emission of **1** and **2** (Figures 3c, S12, S13); it is highly relevant to identify the excitation wavelength that leads to the most intense photoluminescence. In turn, the emission color coordinates are $x = 0.145$; $y = 0.136$ for **1** and $x = 0.153$; $y = 0.053$ for **2**. The fluorescence quantum yields (Φ) are comparable to the monomeric pristine pyrene (0.32);[31] $\Phi = 0.24$ and 0.34 for **1**-*cis* and *trans* and $\Phi = 0.2$ and 0.24 for **2**-*cis* and *trans*, respectively (Table S6).

The concentration-dependent emission of pyrenes has been well documented.[12,13] Already at low concentrations, they tend to form excimers by intermolecular interactions, which are characterized by a broad and red-shifted emission band with low quantum yield.[12,13] Along those lines, we investigated the absorption and emission spectra of the phosphapyrenes at high concentrations. Importantly, we did not observe any changes in neither the absorption nor emission spectra at concentrations as high as 10^{-4} M.[32] In other words, the formation of excimers was prevented by the introduction of phosphorus centers into the pyrenes' core.

The advantage of our synthetic protocol lies in the possibility to introduce phosphorus atoms with two different out-of-plane substituents (i.e. chiral centers) into π-extended systems. Thus, the presence of such phosphorus centers within the phosphapyrene frameworks motivated us to investigate their interaction with polarized light by circular dichroism spectroscopy (CD). Indeed, the inclusion of dissymmetric phosphorus atoms induced an optical response into typically non-active pyrenes. From dichloromethane solutions, the *trans* isomers from both **1** and **2** showed a negative Cotton effect (Figure 4, S14 and S15). Both CD spectra fit quite well

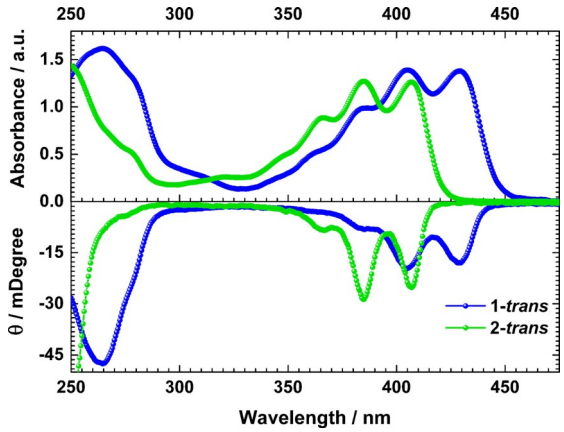

Figure 4. Absorption (up) and CD spectra of **1**-*trans* and **2**-*trans* from DCM solutions.

with their respective absorption features. The ellipticity of **1**-*trans* minimizes at 266, 385, 405 and 428 nm, whereas **2**-*trans* presents minima at 366, 385 and 406 nm. Thus, the insertion of phosphorus atoms into pyrenes' core led to defined molecular packings, modulating the optoelectronic properties, avoiding excimer formations and inducing optical activity.

Once we corroborated the impact of inserting phosphorus atoms into the pyrenes' core, we investigated the possibility to use the out-of-plane oxygen atoms as vector directors to construct 3D architectures by non-covalent interactions. Molecular rings are suitable motifs to verify the directionality of the phosphorus centers. Thus, we designed a proof-of-principle model structure (Figure 5); it consists of two **1**-*cis* molecules—whose oxygen atoms are at the same plane of the main framework—linked by halogen bonds through the 1,4-diiodotetrafluorobenzene (DITFB) (Figure 5). The interaction of such rings along one edge could potentially lead to tubular structures.

The assembly of the molecular rings turned to strongly depend on the employed solvent. Indeed, the use of EtOH and DCM as solvents successfully led to the formation of the experimental model A (Figure 5); i.e., molecular rings, although tilted, with PO···I distances between 2.86 and 3.63 Å.

Intermolecular distances of 3.47 Å between molecular planes (Figure 5) pointed that π-π interactions in the solid state are responsible for such a tilted model. However, the molecular rings did not lead to tubular structures; instead, the latter rings were piling in one axis (see Figure S16). Further investigations with different solvent mixtures revealed that the 3D assembly of the phosphapyrenes could be rearranged into larger and more complex molecular rings by using a mixture of $CHCl_3$ and pentane (Experimental Model B, Figure 5).

Thus, the molecular ring expanded to twelve components bonded by halogen bonds with shorter PO···I distances between 2.87 and 2.91 Å. It is worth noting that the phosphapyrenes interact at the center of the ring through π-π interactions of 3.66 Å from the P-phenyl substituents, forming a lemniscate-like shape (Figure 5, Experimental Model B, top view). Finally, despite the latter lemniscate-like structures did not arrange into the targeted tubular architectures, they organized in the 3D space as well-defined porous architecture through additional intermolecular interactions (Figure 5, Experimental Model B, front view). Thus, the phosphorus centers of the phosphapyrenes may indeed be utilized to control the 3D arrangement through soft halogen bond interactions. As subsequent step, we envisage the possibility to utilize the phosphorus atoms as cornerstone to conceive catenanes but based on covalent bonds. The predicted structure by theoretical calculations is shown in

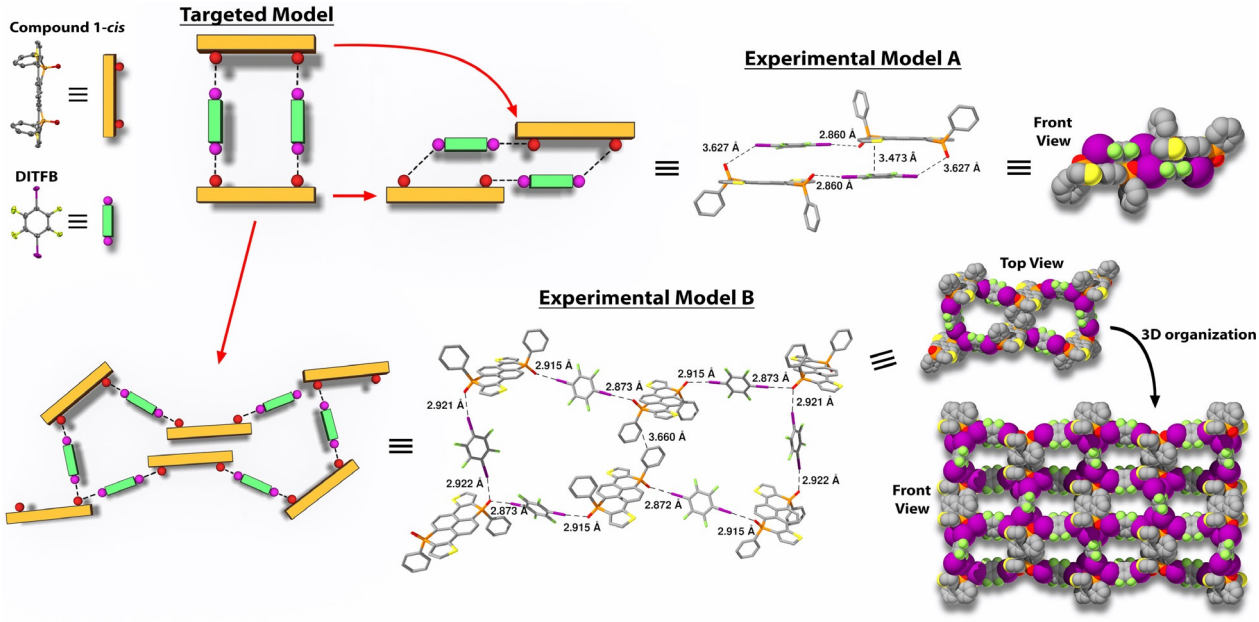

Figure 5. (Top left) Representation of the Targeted Model designed from the **1**-*cis* derivatives and the diiodotetrafluorobezene (DITFB). (Top right) X-ray of the Experimental Model A. (Bottom) Representation and X-ray structure of the Experimental Model B.

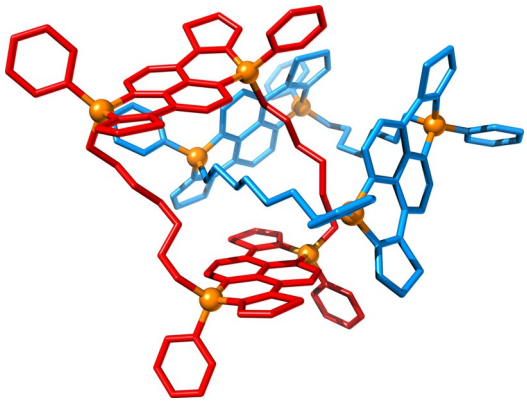

Figure 6. Optimized catenane structure based on molecule **1**-*cis*, built up by quaternization of the phosphorus centers.

Figure 6; the synthesis is currently engaged in our laboratories.

In summary, we describe a strategy to keep control over the 3D arrangement of molecules while providing exciting new properties to π-systems. In particular, we report a synthetic protocol to replace carbon atoms of π-architectures by dissymmetric phosphorus atoms; it allowed to prepare novel, fused phosphapyrene derivatives. The inclusion of dissymmetric phosphorus atoms into pyrenes' core led to the control of the intermolecular interactions avoiding the formation of excimers in solution while maintaining pyrene-pyrene interactions in the solid state. Supported by DFT calculations, the HOMO–LUMO energy gap was reduced compared to pristine pyrenes. As a result, the phosphapyrenes photoluminesce in the visible region of the electromagnetic spectrum with comparable QYs to that of pristine pyrenes. Inserting dissymmetric phosphorus centers into the pyrene' cores induced optical activity. In addition, the presence of the phosphorus atoms converted pyrenes into improved building blocks with the possibility to keep control over their 3D arrangement. In fact, as a proof-of-concept towards more complex architectures, we constructed well-defined molecular rings of different sizes by non-covalent interactions that organized into porous 3D frameworks. Based on our synthetic strategy and discoveries, we envisage the investigation of superior 3D architectures from larger phosphorus-containing π-systems.

Acknowledgements

C.R.-N. and P.H. thank the Organisch-Chemisches Institut of the University of Heidelberg and the UCLM for the support. P.H. thanks the Hanns-Seidel-Stiftung for a fellowship. Financial support from projects RO4899/4-1, SBPLY/17/180501/000518 and RTI2018-101865-A-I00 is gratefully acknowledged. Open access funding enabled and organized by Projekt DEAL.

Conflict of interest

The authors declare no conflict of interest.

Keywords: 3D molecular arrangement · Main group chemistry · optical properties · organophosphorus materials · phosphorus heterocycles

[1] A. Narita, X. Y. Wang, X. Feng, K. Müllen, *Chem. Soc. Rev.* **2015**, *44*, 6616–6643.
[2] W. Ren, H. M. Cheng, *Nat. Nanotechnol.* **2014**, *9*, 726–730.
[3] a) T. Amaya, T. Hirao, *Chem. Rec.* **2015**, *15*, 310–321; b) G. Pacchioni, *Nat. Rev. Mater.* **2017**, *2*, 17062; c) T. Jin, J. Zhao, N. Asao, Y. Yamamoto, *Chem. Eur. J.* **2014**, *20*, 3554–3576.
[4] a) H. F. Bettinger, C. Tonshoff, *Chem. Rec.* **2015**, *15*, 364–369; b) J. E. Anthony, *Angew. Chem. Int. Ed.* **2008**, *47*, 452–483; *Angew. Chem.* **2008**, *120*, 460–492; c) J. L. Marshall, D. Lehnherr, B. D. Lindner, R. R. Tykwinski, *ChemPlusChem* **2017**, *82*, 967–1001; d) M. Watanabe, K. Y. Chen, Y. J. Chang, T. J. Chow, *Acc. Chem. Res.* **2013**, *46*, 1606–1615; e) A. Mateo-Alonso, *Chem. Soc. Rev.* **2014**, *43*, 6311–6324; f) U. H. Bunz, J. U. Engelhart, B. D. Lindner, M. Schaffroth, *Angew. Chem. Int. Ed.* **2013**, *52*, 3810–3821; *Angew. Chem.* **2013**, *125*, 3898–3910; g) U. H. F. Bunz, *Acc. Chem. Res.* **2015**, *48*, 1676–1686.
[5] a) L. Chen, C. Li, K. Müllen, *J. Mater. Chem. C* **2014**, *2*, 1938–1956; b) W. Jiang, Y. Li, Z. Wang, *Acc. Chem. Res.* **2014**, *47*, 3135–3147; c) J. Feng, W. Jiang, Z. Wang, *Chem. Asian J.* **2018**, *13*, 20–30; d) J. Wang, X. Zhan, *New Trends Chem.* **2019**, *1*, 869–881.
[6] a) M. Gingras, *Chem. Soc. Rev.* **2013**, *42*, 968–1006; b) K. Dhbaibi, L. Favereau, J. Crassous, *Chem. Rev.* **2019**, *119*, 8846–8953; c) Y. Shen, C. F. Chen, *Chem. Rev.* **2012**, *112*, 1463–1535; d) M. Gingras, *Chem. Soc. Rev.* **2013**, *42*, 1051–1095; e) M. Gingras, G. Felix, R. Peresutti, *Chem. Soc. Rev.* **2013**, *42*, 1007–1050.
[7] a) K. Shi, J. Y. Wang, J. Pei, *Chem. Rec.* **2015**, *15*, 52–72; b) F. Goubard, F. Dumur, *RSC Adv.* **2015**, *5*, 3521–3551; c) S. A. Wagay, I. A. Rather, R. Ali, *ChemistrySelect* **2019**, *4*, 12272–12288; d) Z. Hua, W. Di, H. L. Sheng, Y. Jun, *Curr. Org. Chem.* **2012**, *16*, 2124–2158.
[8] a) M. S. Lohse, T. Bein, *Adv. Funct. Mater.* **2018**, *28*, 1705553; b) X. Li, C. Yang, B. Sun, S. Cai, Z. Chen, Y. Lv, J. Zhang, Y. Liu, *J. Mater. Chem. A* **2020**, *8*, 16045–16060; c) N. Huang, P. Wang, D. Jiang, *Nat. Rev. Mater.* **2016**, *1*, 16068.
[9] a) R. B. Lin, Y. He, P. Li, H. Wang, W. Zhou, B. Chen, *Chem. Soc. Rev.* **2019**, *48*, 1362–1389; b) I. Hisaki, C. Xin, K. Takahashi, T. Nakamura, *Angew. Chem. Int. Ed.* **2019**, *58*, 11160–11170; *Angew. Chem.* **2019**, *131*, 11278–11288.
[10] a) H. B. Wu, X. W. Lou, *Sci. Adv.* **2017**, *3*, eaap9252; b) L. Chen, X. Zhang, X. Cheng, Z. Xie, Q. Kuang, L. Zheng, *Nanoscale Adv.* **2020**, *2*, 2628–2647; c) J. Meng, X. Liu, C. Niu, Q. Pang, J. Li, F. Liu, Z. Liu, L. Mai, *Chem. Soc. Rev.* **2020**, *49*, 3142–3186.
[11] a) T. M. Figueira-Duarte, K. Müllen, *Chem. Rev.* **2011**, *111*, 7260–7314; b) X. Yang, X. Xu, G. Zhou, *J. Mater. Chem. C* **2015**, *3*, 913–944; c) S. L. Lai, Q. X. Tong, M. Y. Chan, T. W. Ng, M. F. Lo, C. C. Ko, S. T. Lee, C. S. Lee, *Org. Electron.* **2011**, *12*, 541–546; d) D. Chercka, S.-J. Yoo, M. Baumgarten, J.-J. Kim, K. Müllen, *J. Mater. Chem. C* **2014**, *2*, 9083–9086; e) J. K. Salunke, F. L. Wong, K. Feron, S. Manzhos, M. F. Lo, D. Shinde, A. Patil, C. S. Lee, V. A. L. Roy, P. Sonar, P. P. Wadgaonkar, *J. Mater. Chem. C* **2016**, *4*, 1009–1018; f) J. Jayabharathi, P. Jeeva, V. Thanikachalam, S. Panimozhi, *J. Photochem. Photobiol. A* **2017**, *346*, 296–310.
[12] a) G. Bains, A. B. Patel, V. Narayanaswami, *Molecules* **2011**, *16*, 7909–7935; b) V. I. Vullev, H. Jiang, G. Jones, in *Advanced*

Concepts in Fluorescence Sensing: Part B: Macromolecular Sensing (Eds.: C. D. Geddes, J. R. Lakowicz), Springer US, Boston, MA, **2005**, pp. 211 – 239.
[13] a) F. Th, K. Kasper, *Z. Phys. Chem.* **1954**, *1*, 275 – 277; b) S. Karuppannan, J. C. Chambron, *Chem. Asian J.* **2011**, *6*, 964 – 984; c) D. A. Van Dyke, B. A. Pryor, P. G. Smith, M. R. Topp, *J. Chem. Educ.* **1998**, *75*, 615 – 620; d) R. D. Pensack, R. J. Ashmore, A. L. Paoletta, G. D. Scholes, *J. Phys. Chem. C* **2018**, *122*, 21004 – 21017.
[14] a) X. Feng, J. Y. Hu, C. Redshaw, T. Yamato, *Chem. Eur. J.* **2016**, *22*, 11898 – 11916; b) M. M. Islam, Z. Hu, Q. Wang, C. Redshaw, X. Feng, *Mater. Chem. Front.* **2019**, *3*, 762 – 781; c) S. Diring, F. Camerel, B. Donnio, T. Dintzer, S. Toffanin, R. Capelli, M. Muccini, R. Ziessel, *J. Am. Chem. Soc.* **2009**, *131*, 18177 – 18185.
[15] a) J. Yang, Q. Guo, X. Wen, X. Gao, Q. Peng, Q. Li, D. Ma, Z. Li, *J. Mater. Chem. C* **2016**, *4*, 8506 – 8513; b) J. Yang, L. Li, Y. Yu, Z. Ren, Q. Peng, S. Ye, Q. Li, Z. Li, *Mater. Chem. Front.* **2017**, *1*, 91 – 99.
[16] a) P. Sonar, M. S. Soh, Y. H. Cheng, J. T. Henssler, A. Sellinger, *Org. Lett.* **2010**, *12*, 3292 – 3295; b) Y.-J. Pu, M. Higashidate, K.-i. Nakayama, J. Kido, *J. Mater. Chem.* **2008**, *18*, 4183 – 4188; c) S. Bernhardt, M. Kastler, V. Enkelmann, M. Baumgarten, K. Müllen, *Chem. Eur. J.* **2006**, *12*, 6117 – 6128; d) M. Gingras, V. Placide, J. M. Raimundo, G. Bergamini, P. Ceroni, V. Balzani, *Chem. Eur. J.* **2008**, *14*, 10357 – 10363.
[17] S. S. Chissick, M. J. S. Dewar, P. M. Maitlis, *Tetrahedron Lett.* **1960**, *1*, 8 – 10.
[18] a) T. Baumgartner, R. Reau, *Chem. Rev.* **2006**, *106*, 4681 – 4727; b) T. Baumgartner, *Acc. Chem. Res.* **2014**, *47*, 1613 – 1622.
[19] a) E. Regulska, P. Hindenberg, C. Romero-Nieto, *Eur. J. Inorg. Chem.* **2019**, 1519 – 1528; b) P. Hindenberg, C. Romero-Nieto, *Synlett* **2016**, *27*, 2293 – 2300; c) M. A. Shameem, A. Orthaber, *Chem. Eur. J.* **2016**, *22*, 10718 – 10735; d) G. Pfeifer, F. Chahdoura, M. Papke, M. Weber, R. Szucs, B. Geffroy, D. Tondelier, L. Nyulászi, M. Hissler, C. Müller, *Chem. Eur. J.* **2020**, *26*, 10534 – 10543; e) E. Regulska, C. Romero-Nieto, *Dalton Trans.* **2018**, *47*, 10344 – 10359.
[20] O. Larrañaga, C. Romero-Nieto, A. de Cózar, *Chem. Eur. J.* **2019**, *25*, 9035 – 9044.
[21] a) J. R. Brandt, F. Salerno, M. J. Fuchter, *Nat. Rev. Chem.* **2017**, *1*, 0045; b) D.-Y. Kim, *J. Korean Phys. Soc.* **2006**, *49*, 505 – 508; c) R. Farshchi, M. Ramsteiner, J. Herfort, A. Tahraoui, H. T. Grahn, *Appl. Phys. Lett.* **2011**, *98*, 162508.
[22] C. Romero-Nieto, A. Lopez-Andarias, C. Egler-Lucas, F. Gebert, J. P. Neus, O. Pilgram, *Angew. Chem. Int. Ed.* **2015**, *54*, 15872 – 15875; *Angew. Chem.* **2015**, *127*, 16098 – 16102.
[23] a) S. Bensaid, J. Roger, K. Beydoun, D. Roy, H. Doucet, *Synth. Commun.* **2011**, *41*, 3524 – 3531; b) J. Zhao, L. Huang, K. Cheng, Y. Zhang, *Tetrahedron Lett.* **2009**, *50*, 2758 – 2761; c) M. H. Daniels, J. R. Armand, K. L. Tan, *Org. Lett.* **2016**, *18*, 3310 – 3313.
[24] Note that the investigation of the particular reaction mechanism goes beyond the scope of this article; it deserves a multidisciplinary study on its own, which will be published elsewhere.
[25] a) P. Hindenberg, F. Rominger, C. Romero-Nieto, *Chem. Eur. J.* **2019**, *25*, 13146 – 13151; b) P. Hindenberg, M. Busch, A. Paul, M. Bernhardt, P. Gemessy, F. Rominger, C. Romero-Nieto, *Angew. Chem. Int. Ed.* **2018**, *57*, 15157 – 15161; *Angew. Chem.* **2018**, *130*, 15377 – 15381; c) P. Hindenberg, A. López-Andarias, F. Rominger, A. de Cózar, C. Romero-Nieto, *Chem. Eur. J.* **2017**, *23*, 13919 – 13928.
[26] A. Belyaev, Y. T. Chen, Z. Y. Liu, P. Hindenberg, C. H. Wu, P. T. Chou, C. Romero-Nieto, I. O. Koshevoy, *Chem. Eur. J.* **2019**, *25*, 6332 – 6341.
[27] The reversibility was corroborated at different scan rates.
[28] V. D. Parker, *J. Am. Chem. Soc.* **1976**, *98*, 98 – 103.
[29] N. P. E. Barry, B. Therrien, in *Organic Nanoreactors* (Ed.: S. Sadjadi), Academic Press, Boston, **2016**, pp. 421 – 461.
[30] K. Ahmed, A. Auni, G. Ara, M. M. Rahman, M. Y. A. Mollah, M. A. B. H. Susan, *J. Bangladesh Chem. Soc.* **2013**, *25*, 146 – 158.
[31] I. B. Berlman, in *Handbook of Fluorescence Spectra of Aromatic Molecules, Second Edition* (Ed.: I. B. Berlman), Academic Press, San Diego, **1971**, pp. 67 – 95.
[32] This is in line with the behaviour of phosphorous/nitrogen-fused pyrene derivatives: C. L. Deng, J. P. Bard, L. N. Zakharov, D. W. Johnson, M. M. Haley, *Org. Lett.* **2019**, *21*, 6427 – 6431.

Manuscript received: August 19, 2020
Accepted manuscript online: September 28, 2020
Version of record online: November 3, 2020

